

A

| | | | |
|-----------------------------|------|--|------|
| TET1 (<i>H. sapiens</i>) | 1654 | EGRPFSGV T ACLDFC AHP HRD I HNMNNGSTV | 1684 |
| TET1 (<i>M. musculus</i>) | 1634 | EGRPFSGV T CCMDFC AHS HKD I HNMHNGSTV | 1664 |
| TET2 (<i>H. sapiens</i>) | 1364 | EGRPFSGV T ACLDFC AHA HRD L HNMQNGSTL | 1394 |
| TET2 (<i>M. musculus</i>) | 1277 | EGRPFSGV T ACLD FSAHS HRD Q QNMPNGSTV | 1317 |

T1372 (hTET2) Fe(II)-binding HxD Motif

| TET Activity | mTET1 | mTET2 |
|----------------|--------|--------|
| Normal | WT | WT |
| Low Efficiency | T1642A | T1285A |
| 5hmC Stalling | T1642V | T1285E |
| Inactive | HxD | HxD |

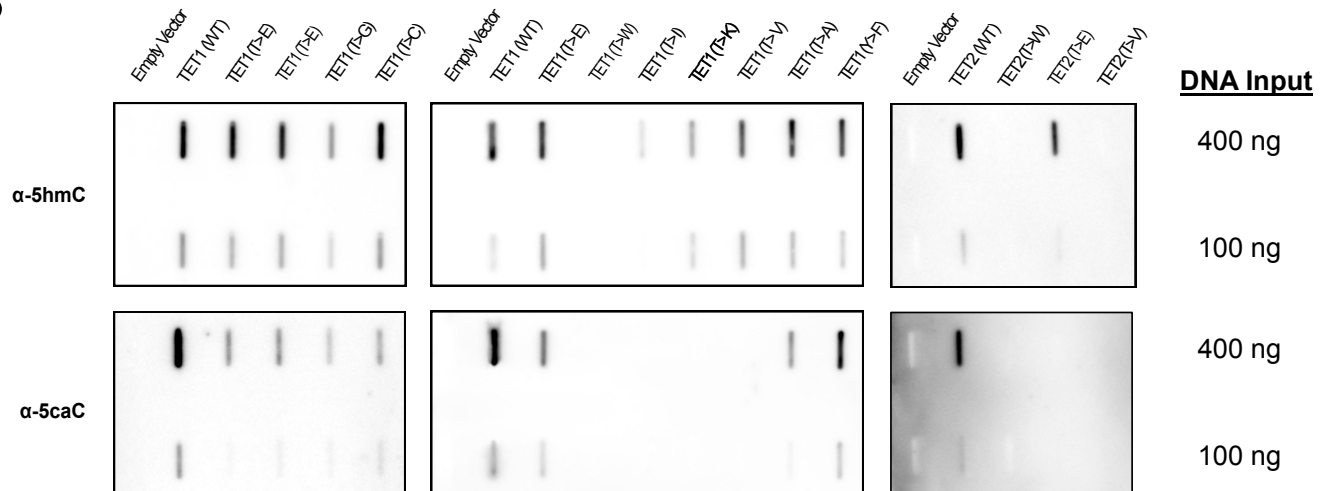
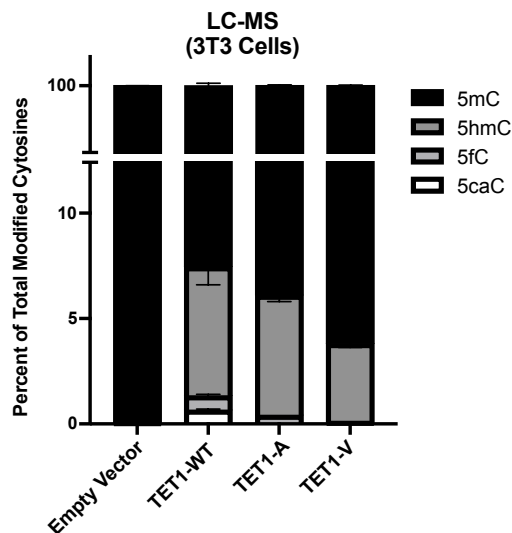
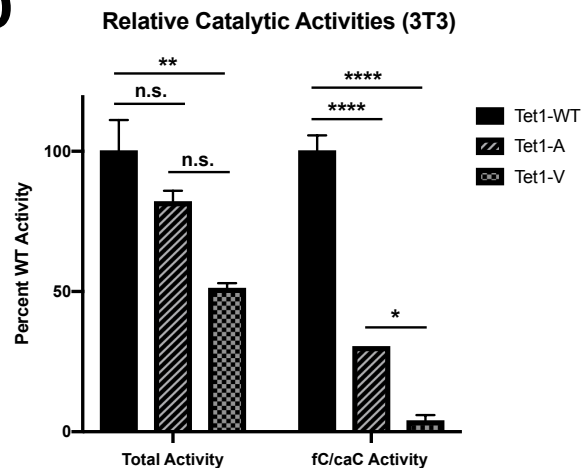
B**C****D**

Figure S1 related to Figure 1. (A) Alignment of human and mouse TET1 and TET2 protein sequences (human TET2 T1372 site and Fe(II)-binding HxD motif indicated by red boxes) with summary of mouse TET1 and TET2 mutants used in this study. **(B)** Representative slot blots for 5hmC and 5caC in genomic DNA isolated from HEK cells transfected with a broader array of TET1 or TET2 catalytic variants. TET1 variants carry mutations at either T1642 (E, G, C, W, I, K, V, A) or Y2049F, while TET2 variants carry mutations at T1285 (W, E, V). **(C)** Genomic levels of modified cytosines in transfected NIH3T3 cells, quantified by LC-MS/MS and expressed as the percentage of total modified cytosines present in each sample (mean \pm SEM; $n=2-4$). **(D)** Relative catalytic activities of TET1 variants. Modified cytosines were normalized to their mean levels in cells transfected with WT TET1 to determine the relative catalytic activities of each variant. Relative catalytic activities are presented as either total TET activity (5hmC + 5fC + 5caC) or fC/caC activity (mean relative catalytic activities \pm SEM; $n=2-3$; one-way ANOVA with Tukey multiple comparisons; n.s. = not significant; * $p < 0.05$; ** $p < 0.01$; *** $p < 0.001$; **** $p < 0.0001$).

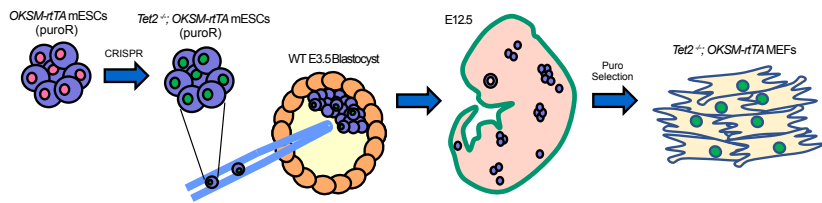
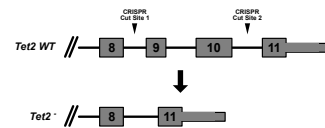
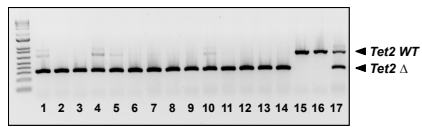
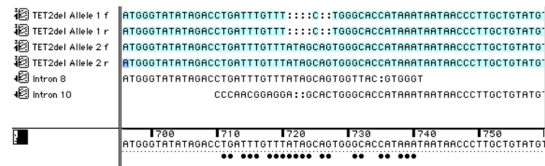
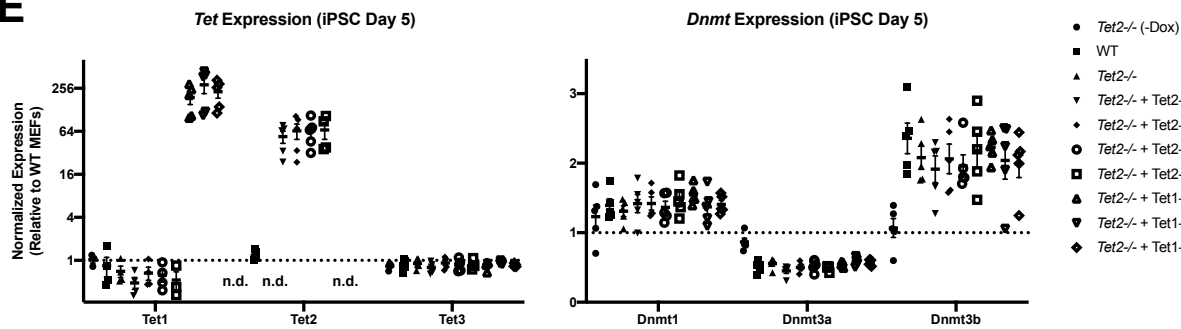
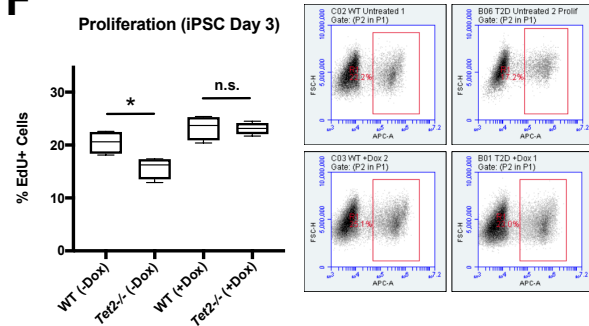
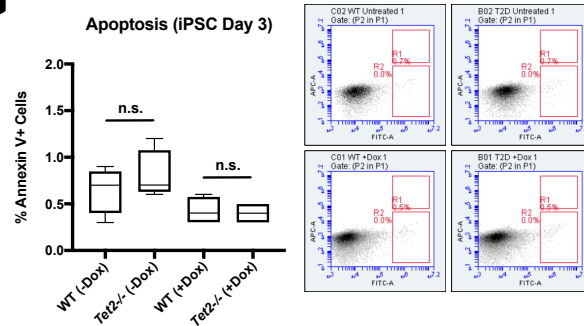
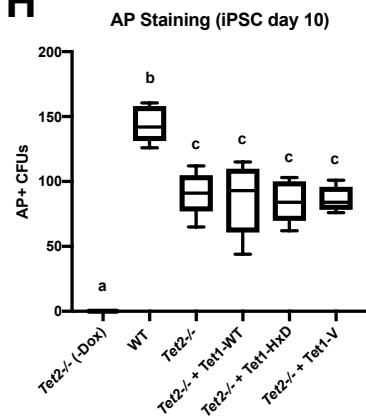
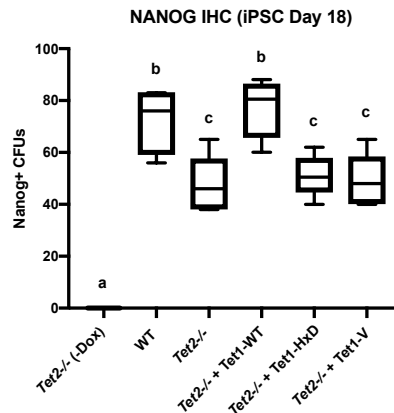
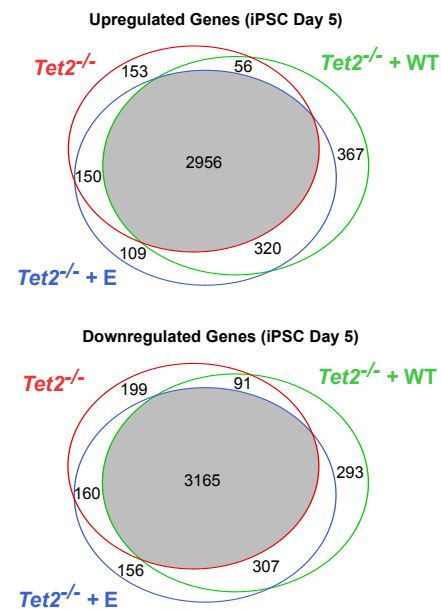
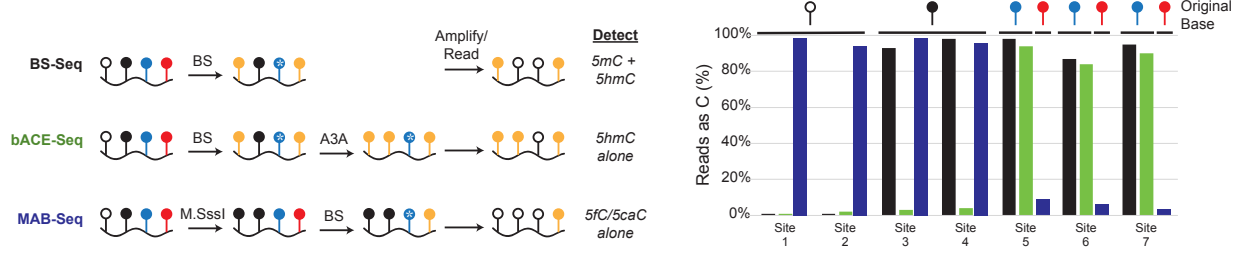
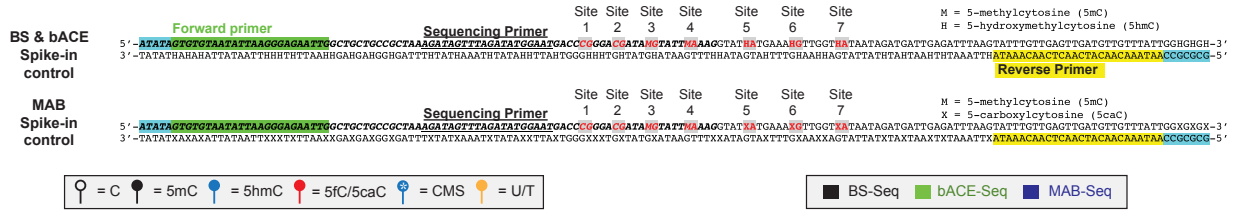
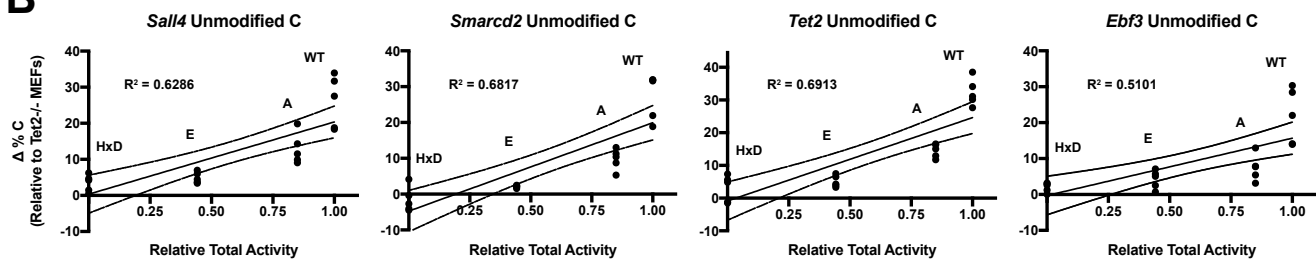
A**B****C****D****E****F****G****H****I****J**

Figure S2 related to Figure 2. (A) Outline of *Tet2*^{-/-}; *OKSM-rtTA* MEF derivation procedure. Wild-type, Dox-inducible *OKSM-rtTA* mouse ESCs (mESCs) were subjected to CRISPR-Cas9 mutagenesis to delete both endogenous alleles of *Tet2*. The resultant *Tet2*^{-/-}; *OKSM-rtTA* mESCs were subcloned and injected into mouse embryonic day 3.5 (E3.5) blastocysts to generate chimeric embryos. Embryos were transferred to pseudopregnant dams and allowed to develop to E12.5, at which point they were harvested and processed for MEF isolation. Pure *Tet2*^{-/-}; *OKSM-rtTA* MEF cultures were obtained through puromycin selection. **(B)** CRISPR-Cas9 mutagenesis strategy for *Tet2* knockout. Double-stranded breaks at the indicated cut sites and subsequent non-homologous end-joining (NHEJ) results in the excision of exons 9 and 10 of the *Tet2* catalytic domain. **(C)** Genotyping PCR assay for *Tet2* in *Tet2*^{-/-}; *OKSM-rtTA* MEFs following 48 hours of puromycin selection. Lanes 1-14 represent MEF clones derived from individual chimeric embryos, while lanes 15-17 represent WT (clones 15, 16) and heterozygous (clones 17) *Tet2*^{+/-} mESC samples. Clones 2, 13, and 14 were used for all subsequent experiments. **(D)** Forward (f) and reverse (r) sequencing of *Tet2* in *Tet2*^{-/-}; *OKSM-rtTA* MEF clone 14. Note the fusion of *Tet2* introns 8 and 10 resulting from CRISPR/Cas9 NHEJ, as well as the presence of two distinct mutagenized alleles. **(E)** qRT-PCR for *Tet* (left) and *Dnmt* (right) expression relative to untreated WT MEFs after 5 days of Dox treatment. Cells were retrovirally transduced with either empty vector or the indicated *Tet1* or *Tet2* variant. Expression levels were normalized to *Nono*. Data points represent independent experiments, with mean expression levels +/- SEM indicated (n=5; n.d. = not detected). **(F)** EdU labelling of WT and *Tet2*^{-/-} MEFs either untreated (-Dox) or following 3 days of Dox treatment. Box plots indicate median percentage of EdU⁺ cells for each condition (one-way ANOVA with Sidak's multiple comparisons; *p < 0.05; n.s. = not significant; n=4). Representative sorting plots for each condition are included on the right (EdU⁺ cells indicated by the red box). **(G)** Annexin V labelling of apoptotic WT and *Tet2*^{-/-} MEFs either untreated (-Dox) or following 3 days of Dox treatment. Box plots indicate median percentage of Annexin V⁺ cells for each condition (one-way ANOVA with Sidak's multiple comparisons; n=4). Representative sorting plots for each condition are included on the right (Annexin V⁺ cells indicated by the lower-right red box). **(H)** Alkaline phosphatase (AP) staining of pluripotent colonies after 10 days of Dox treatment for TET1-transduced cells. Box plots indicate median AP⁺ colony forming units (CFUs) for each treatment group, with letters designating statistically distinct groups (one-way ANOVA with Tukey multiple comparisons; n=5). **(I)** Immunohistochemistry for Nanog-positive stable pluripotent colonies after one week of Dox withdrawal (median Nanog⁺ CFU counts; one-way ANOVA with Tukey multiple comparisons; n=5). **(J)** Venn overlap of differentially expressed genes following 5 days of Dox treatment relative to untreated *Tet2*^{-/-} MEFs (RNA-seq; n=3-4; FDR < 0.05; fold-change > 1.5).

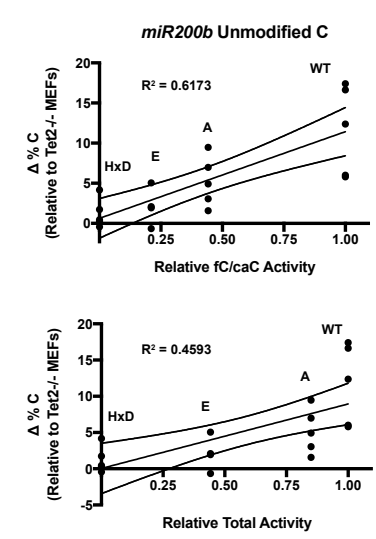
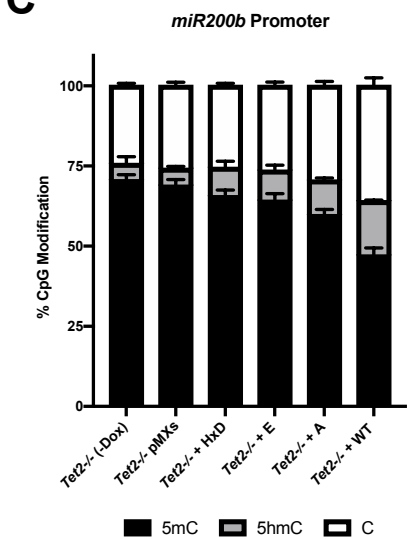
A



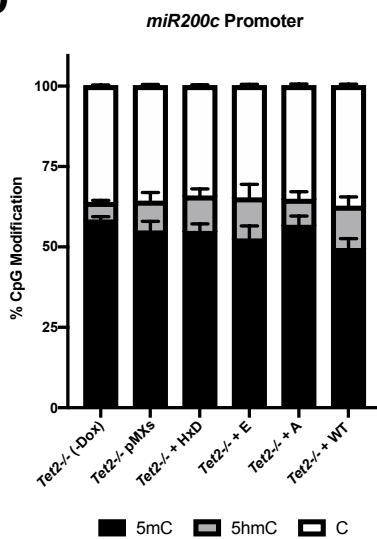
B



C



D



E

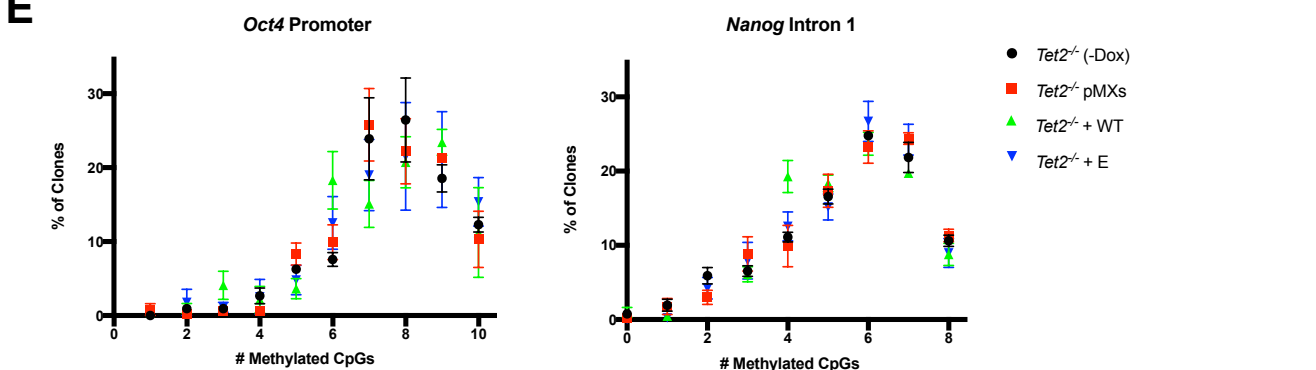


Figure S3 related to Figure 3. (A) bACE- and MAB-Seq conversions of PCR-generated spike-in controls. The spike-ins were generated by PCR amplification of a template using a spike-in generation forward primer (bold sequence), which contains 5mC, a reverse primer, and the 5hmCTP or 5caCTP in lieu of dCTP. After bisulfite (BS), bisulfite + APOBEC3A (bACE), or M.Sssl + bisulfite (MAB) treatment, the products were amplified using forward and reverse primers. Pyrosequencing with the indicated sequencing primer was then used to analyze the number of C versus T reads at each site. In the bACE-Seq reaction, unmodified cytosines are fully deaminated following bisulfite reaction (site 1 and site 2). 5mC bases are resistant to deamination (site 3 and site 4), and 5hmC bases are converted into 5-methylenesulfonate (CMS, sites 5-7 of the bACE spike-in). Following APOBEC3A treatment, 5mCs are now subjected to deamination while the original 5hmC bases, converted to CMS, are protected from deamination. In the MAB-Seq reaction, unmodified cytosines are first converted to 5mC by M.Sssl, thereby protecting them from deamination by bisulfite. Following bisulfite treatment, only 5fC or caC (sites 5-7 of the MAB spike-in) are deaminated. **(B)** Alternative model for TET2 activity at the *Sall4*, *Smarcd2*, *Tet2*, and *Ebf3* reprogramming enhancers. Data points represent independent experiments plotted against total TET2 activity (5hmC + 5fC + 5caC) values determined from HEK overexpression experiments (Fig. 1C). Simple linear regressions were performed for each enhancer, with the line of best fit (solid) and 95% confidence intervals (dotted) indicated (n=4-5). **(C-D)** Relative levels of unmodified cytosine, 5hmC, and 5mC at the **(C)** miR200b and **(D)** miR200c cluster promoters in untreated *Tet2*^{-/-} MEFs or following 5 days of Dox treatment. Cells were retrovirally transduced with empty vector or the indicated *Tet2* variant. For the right panel of **(C)**, data points represent independent experiments plotted against either the relative fC/caC or total activity values determined from HEK overexpression experiments (Fig. 1C). Simple linear regressions were performed, with the line of best fit (solid) and 95% confidence intervals (dotted) indicated. (n=4-5). **(E)** Relative proportions of bisulfite clonotypes at the *Oct4* promoter and *Nanog* intron 1 in untreated *Tet2*^{-/-} MEFs or following 5 days of Dox treatment, as determined by bisulfite sequencing. Data points represent the mean percentage of clones with the indicated clonotype +/- SEM (n=3-4). Trending increases were observed in the proportion of lowly methylated clones (< 5 methylated CpGs) in *Tet2*-WT cells.

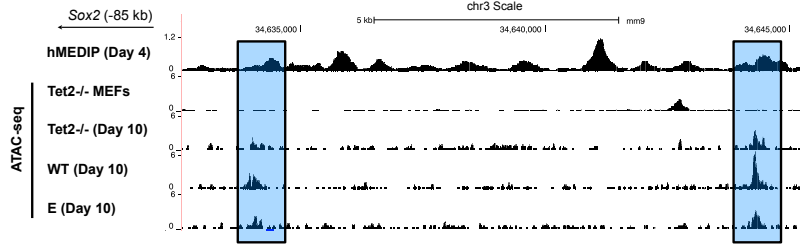
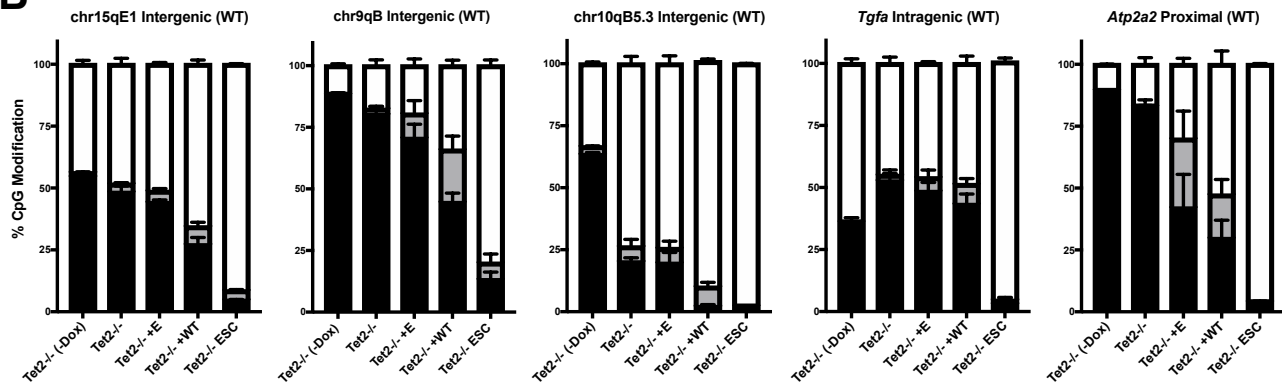
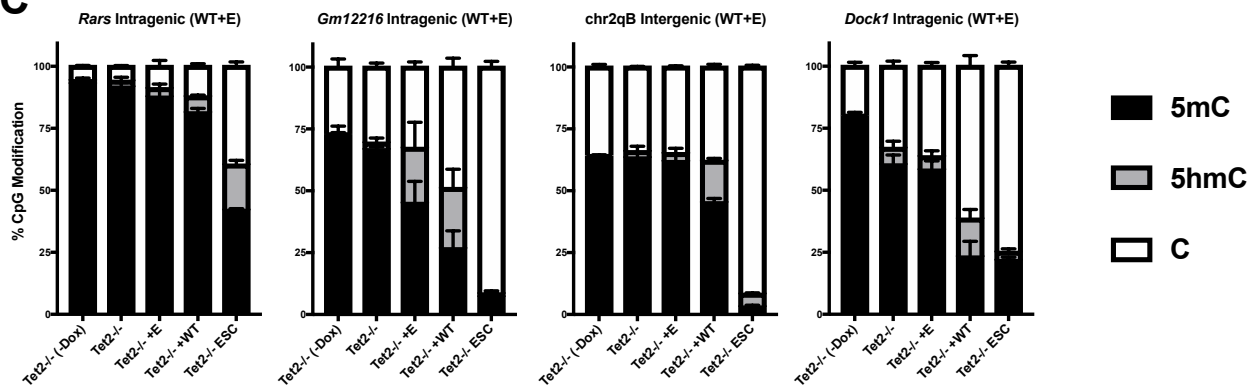
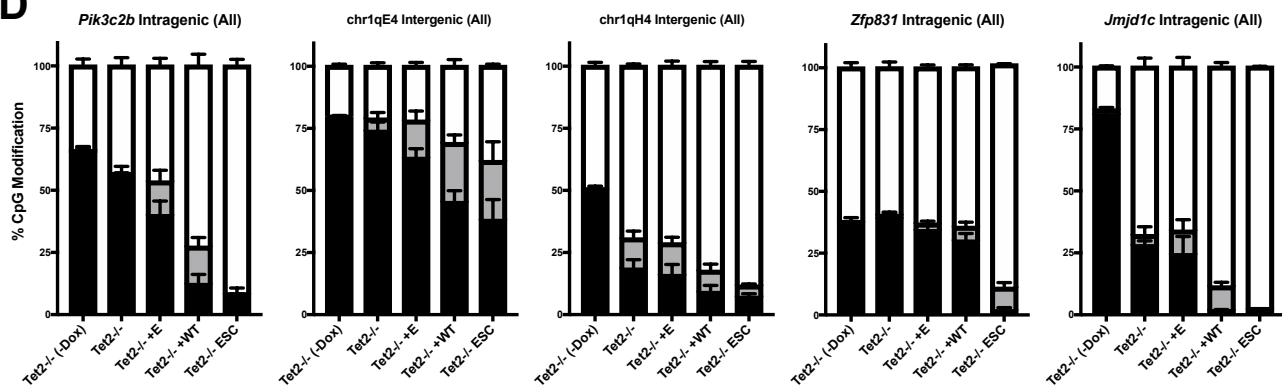
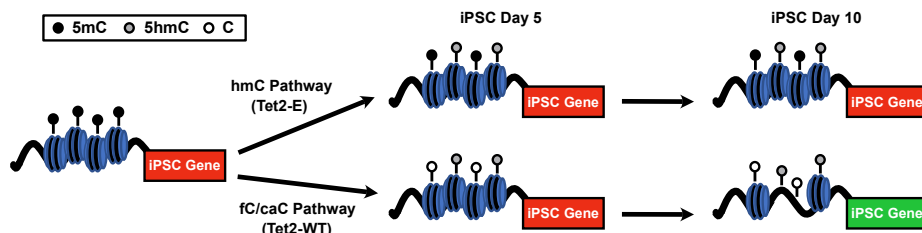
A**B****C****D****E**

Figure S4 related to Figure 4. (A) Differential ATAC peaks overlapping 5hmC signal at two distal Sox2 enhancers. UCSC genome browser snapshots include ATAC signal (merge of 4 biological replicates) for each condition at reprogramming day 10, as well as hMeDIP signal at iPSC day 4 (Sardina et al., 2018). Direction and distance to Sox2 are indicated by the arrow in the top-left corner. **(B-D)** Relative levels of unmodified cytosine, 5hmC, and 5mC at regions showing **(B)** WT-specific (WT), **(C)** WT- or E-specific (WT+E), or **(D)** shared (All) iPSC ATAC peaks overlapping 5hmC signal. The relative levels of each cytosine derivative were measured in untreated *Tet2*^{-/-} MEFs (-Dox), untreated *Tet2*^{-/-} mESCs, or *Tet2*^{-/-} MEFs following 5 days of Dox treatment. Cells were retrovirally transduced with empty vector or the indicated *Tet2* variant. Bar graphs represent the mean percentage of each cytosine derivative +/- SEM (n=4). **(E)** Model for fC/caC pathway's role in iPSC reprogramming. In contrast to the hmC pathway, the fC/caC pathway drives significant DNA demethylation during the early stages of iPSC reprogramming. This demethylation facilitates chromatin opening at these loci at later iPSC stages, thereby generating active chromatin environments in regions critical for the reprogramming process.

| Expression vectors for HEK/3T3 transfections |
|---|
| Tet1-CD WT pLEXm |
| Tet1-CD T1642E pLEXm |
| Tet1-CD T1642V pLEXm |
| Tet1-CD T1642A pLEXm |
| Tet1-CD T1642G pLEXm |
| Tet1-CD T1642C pLEXm |
| Tet1-CD T1642W pLEXm |
| Tet1-CD T1642I pLEXm |
| Tet1-CD T1642K pLEXm |
| Tet1-CD Y2049F pLEXm |
| Tet2-CD WT pLEXm |
| Tet2-CD T1285E pLEXm |
| Tet2-CD T1285A pLEXm |
| Tet2-CD T1285W pLEXm |
| Tet2-CD T1285V pLEXm |
| Retroviral vectors |
| Tet1-CD WT pMXs |
| Tet1-CD WT pMXs |
| Tet1-CD HxD pMXs |
| Tet2-CD WT pMXs |
| Tet2-CD T1285E pMXs |
| Tet2-CD T1285A pMXs |
| Tet2-CD HxD pMXs |
| CRISPR/Cas9 Vectors |
| Tet2 Int8a pX330 |
| Tet2 Int10a pX330 |

Table S1 related to STAR Methods.